Received August 2004
Revised April 2005
Accepted April 2005

Three dimensional numerical simulation and analysis of the airside performance of slotted fin surfaces with radial strips

Jun-Jie Zhou and Wen-Quan Tao
School of Energy and Power Engineering, Xi'an Jiaotong University, Shananxi, People's Republic of China

Abstract

Purpose – To provide some heat transfer and friction factor results for fin-and-tube heat transfer surfaces which may be used in air conditioning industry.

Design/methodology/approach – Numerical simulation approach was adopted to compare the plain plate fin and three types of radial slotted fin surfaces.

Findings – It is found that at the same frontal velocity (1.0-3 m/s) the plain plate fin has the lowest heat transfer rate with the smallest pressure drop. The full slotted fin surface has the highest heat transfer rate with the largest pressure drop penalty. The partially slotted fin (where the strips are mainly located in the rear part of the fin) and the back slotted fin are some what in between. Under the identical pumping power constraint, the partially slotted fin surface behaves the best.

Research limitations/implications – The results are only valid the two-row fin surface.

Practical implications – The results are very useful for the design of two-row tube fin surfaces with high efficiency.

Originality/value – This paper provides original information of slotted fin surface with radial strips from the field synergy principle.

Keywords Numerical analysis, Simulation, Heat transfer, Heat exchangers

Paper type Research paper

Nomenclature

A_0, A_1, A_2	= curve-fitting parameter	Q	= heat transfer rate
Dp	= pressure drop	Re	= Reynolds number
f	= friction factor	θ_m	= average synergy angle
Int	= integrated value of convective term	d	= fin collar outside diameter of tube
Nu	= Nusselt number	h	= average heat transfer coefficient

1. Introduction

Finned-tube heat exchangers have been widely used in air-conditioning, refrigeration, chemistry engineering and power industries. Various types of finned surfaces are proposed, including the wavy or corrugated fin, offset strip fin and louver fin

Engineering Computations: International Journal for Computer-Aided Engineering and Software
Vol. 22 No. 8, 2005
pp. 940-957

0264-4401
DOI 10.1108/02644400510626497

This work was supported by the Research Fund of Doctorial Project of China (RFDP20030698015) and the National Natural Science Foundation of China (No. 50476046).

(Leu *et al.*, 2001; Atkinson *et al.*, 1998; Jing, 2001; Comini and Groce, 2001; Zhou *et al.*, 2003), etc. The finned surfaces are almost exclusively adopted for air-side heat transfer in compact heat exchangers for which the most comprehensive design database up to the eighties of twentieth century is the monograph by Kays and London (1984). Numerous experimental investigations (Mori and Nakayama, 1982; Xin *et al.*, 1992; Wang *et al.*, 2001) have shown that for enhancing heat transfer the interrupted fin surfaces behave better than the corrugated fin surfaces because they can provide periodical renewal of the boundary layer from the conventional understanding of heat transfer enhancement mechanism. For example, it was shown by Xin *et al.* (1992) that according to their test results under the same pumping power the slotted fin surface of two-row plate-fin-and-tube surface is about 40 percent higher than that of plain plate fin and than wavy fin surface. Numerical simulations have also been widely used to investigate the flow and heat transfer details of different kinds of plate-fin-and-tube surfaces. Shah *et al.* (2001) made a comprehensive review on the numerical simulations for many finned heat transfer surfaces.

Recently, Guo *et al.* (1998) and Wang *et al.* (1998) proposed a new concept of enhancing convective heat transfer for boundary layer type flow. According to this concept the heat transfer flux at the wall equals the integration of the inner production of $\rho c_p(\vec{U} \bullet \mathrm{grad} T)$ along the boundary layer thickness. Therefore, for a fixed flow rate and temperature difference the smaller the intersection angle (hereafter, it will be called synergy angle) between the velocity and temperature difference, the larger the heat transfer flux. This implies that the reduction of the intersection angle will increase the convective heat transfer rate. Later this new concept has been extended to the elliptical type flow (Tao *et al.*, 2002a). It is shown that for conventional fluids such as air and water, the integration:

$$\int_{\Omega} \rho c_p(\vec{U} \bullet \mathrm{grad} T)\, \mathrm{d}\Omega$$

represents the heat transfer rate over the entire domain. And it has also been demonstrated by numerical simulations that all the existed explanations for enhancing convective heat transfer can be unified under this principle (Tao *et al.*, 2002b). This basic idea is now called the field synergy principle. Thus, it is clear that a better synergy (i.e. smaller synergy angle between the velocity and temperature gradient) will make the integration larger, hence, enhance the heat transfer.

In this paper, the heat transfer and pressure drop characteristics are numerically investigated for four types of fin surfaces, including plain plate fin and three-slotted fin surfaces at which the slots are arranged more or less in the radial direction. The effect of finite thickness of the fin is taken into account. The numerical results are discussed from the point of view of the field synergy principle, and the effect of slot locations on heat transfer and pressure drop is analyzed in detail.

2. Computational models

A schematic diagram of the plain plate-fin-and-tube surface is shown in Figure 1. In this paper, plate fin and tube surface with two rows of tubes in the flow direction is studied. The slotted fin surface is alike except that there are some slotted strips in the plain plate.

Figure 2 shows the detail fin configurations of the four type fin patterns studied among whom three fin surfaces are slotted with different arrangement of slots.

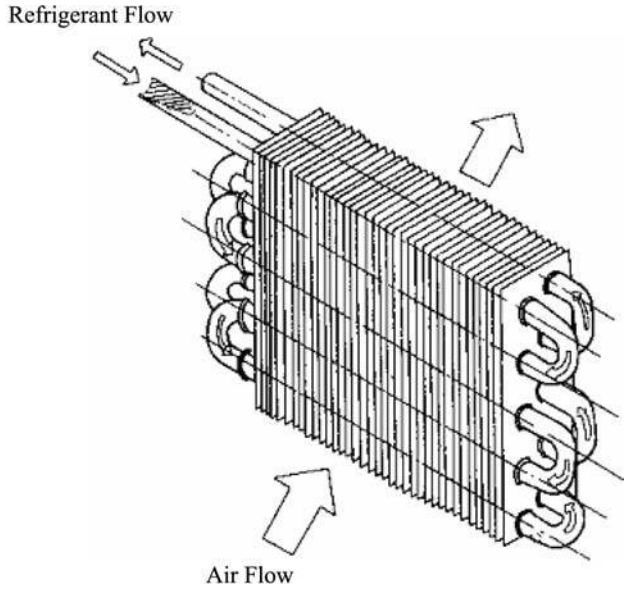

Figure 1.
Schematic diagram of fin-and-tube heat exchanger

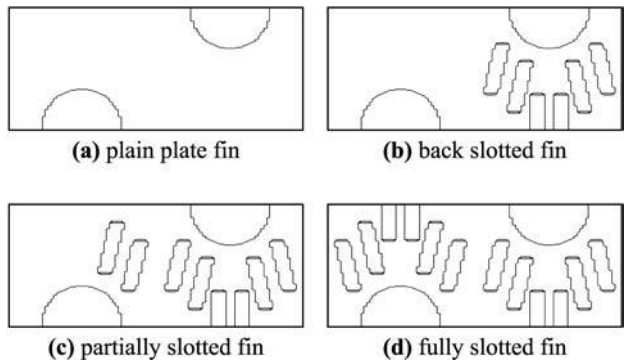

Figure 2.
Four types of fin surfaces

Figure 2(a) is the plain plate fin. Figure 2(b) is a slotted fin surface with six strips mainly located in the back part along the flow direction. Each strip is punched with 1 mm width and 0.6 mm depths from the base sheet and is aligned more or less in the radial direction of the second tube. The strip number of Figure 2(c) is eight with two more strips located in the front part of the fin surface. In Figure 2(d) the entire fin surface is slotted and there 12 strips with each tubes share six ones. The fins are made of aluminum and the tubes of copper. The detailed geometry of the heat exchanger surface and operating conditions are presented in Table I.

Following assumptions are adopted:

- the fluid flow is in steady state and laminar;
- the thermal physical properties are constant and the energy dissipation is neglected;

Tube outside diameter	7.2 mm
Longitudinal tube pitch	12.7 mm
Transverse tube pitch	10.5 mm
Fin thickness	0.105 mm
Fin pitch	1.2 mm
Slotted Strip width	1.0 mm
Radial angle	77.2°
Slit height	0.6 mm
Tube temperature	313 K
Inlet air temperature	303 K
Inlet frontal velocity	1.0-3.0 m/s

Table I.
Operating conditions and geometry dimension

- the contact between the fin surface and tube is perfect;
- in the tube axis direction, there are many pieces of fin surface, hence, the fluid flow and heat transfer are periodically developed in that direction, and the heat transfer and fluid flow between any two pieces of fin surfaces can serve as a representation of the whole stack of surface; and
- in the spanwise direction, tubes are periodically arranged such that the fluid flow and heat transfer are also periodically developed in this direction.

With these assumptions, our computational domain is shown in Figure 3 for one of the slotted fin surface. The three coordinates x, y, and z are in main flow direction, spanwise direction and perpendicular to the fin sheet, respectively. For this computational domain, following two features may be noted. First the height of the computational domain is the fin pitch, and half thickness of the upper and lower fin sheet is included in the computational domain. This implies that the computation is of conjugated type in that both the fin and fluid temperature distributions are simultaneously determined. Second, the fluid flows across the fin from the left to the right. Ahead of the first tube and at the back of the second tube there are additional regions where no fin sheet exists. The streamwise length of these two additional regions are 1.5 and 5 times of the streamwise fin length, respectively. Therefore, the whole length of the computation domain is 7.5 times of the real fin length.

Because of space limit, the 3D general governing equation in Cartesian coordinates will not be given here, and for details reference (Patankar, 1980) may be consulted.

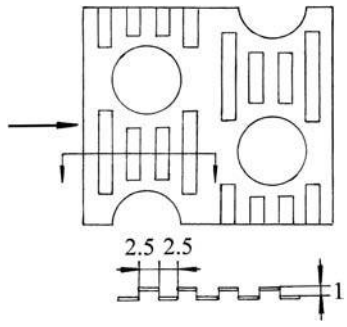

Figure 3.
Slotted fin surface with parallel strips

The boundary conditions are as follows:

- inlet boundary: $u = \text{const}$, $v = w = 0$, $T_{\text{in}} = \text{const}$.
- outlet boundary:

$$\frac{\partial u}{\partial x} = \frac{\partial v}{\partial x} = \frac{\partial w}{\partial x} = 0, \quad \frac{\partial T}{\partial x} = 0.$$

- top and bottom boundary: in the extended region,

$$\frac{\partial u}{\partial z} = \frac{\partial v}{\partial z} = 0, \quad w = 0;$$

  In the fin region, periodic boundary condition is applied in the place where slit exists: $u(x,y,0) = u(x,y,p_f)$, $v(x,y,0) = v(x,y,p_f)$, $w(x,y,0) = w(x,y,p_f)$, $T(x,y,0) = T(x,y,p_f)$; In the remaining place, adiabatic boundary condition is adopted for temperature at the symmetric line of the fin thickness, isothermal condition for temperature is used for the tube boundary, while all velocities take zero; and

- frontal and back boundary:

$$\frac{\partial u}{\partial y} = \frac{\partial v}{\partial y} = 0, \quad w = 0, \quad \frac{\partial T}{\partial y} = 0$$

for the fluid region, and at the tube wall surface $T = \text{const}$, $u = v = w = 0$ are set up.

The governing equations were discretized by FVM (Patankar, 1980; Tao, 2001), and the SIMPLE algorithm was used. The techniques described in Tao (2001, 2000) were used to numerically implement the conjugated solution procedure.

3. Examination of model and grid independency

Some preliminary computations were conducted to verify the model and the grid-independence of the numerical solutions. For this end the slotted fin surface with strips parallel to the y-axis was simulated for which experimental correlation is available in the open literature (Kang *et al.*, 1994). The fin surface simulated is shown in Figure 3. The computational domain is similar to the one shown in Figure 2 and only the fin part shown in Figure 4. Some geometric data of the fin are as follows: fin thickness is 0.2 mm, the outer diameter of tube is 10.15 mm, and the fin pitch is 2.0 mm. Three grid systems were used with total grid number of 1.8×10^5, 3.2×10^5, and 4.5×10^5, respectively. The convergence criterion is the relative residual of the

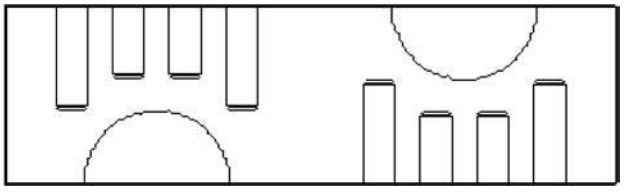

Figure 4.
Slotted fin with parallel strips

momentum equations: $R_m \leq 5 \times 10^{-6}$. It is found that the maximum relative difference of the average Nusselt number and friction factor of the three grid systems is 3.7 and 2.8 percent, respectively. Since this difference is not quite small, the grid system with the intermediate grid number, (i.e. 3.2×10^5) was adopted for computations. The simulated Nusselt numbers are then compared with the experimental correlation of Kang *et al.* (1994) at the approaching velocities from 0.5 to 1.5 m/s, typical values in the air-conditioning engineering. The comparison results are listed in Table II. Except from the Nusselt number at the approaching velocity of 0.5 m/s, the agreements of all the other data are reasonably good, with deviations usually less than 10 percent. Such deviations of the numerical results from experimental correlation are acceptable. The most severe deviation is in Nusselt number at the approaching velocity of 0.5 m/s. According to Kang *et al.* (1994), at the low approaching velocity, the heat transfer rate measurement accuracy was deteriorated, and it is our consideration that this rather large deviation may be caused by the test data uncertainty.

With this success in experimental validation, we have sufficient confidence to explore the heat transfer and fluid flow characteristics of the air flow in the slotted fin-tube passages.

In the computations for the slotted fin surfaces with radial strips, the grid number is 3.786×10^5 ($136 \times 116 \times 24$) in order to match the boundaries of the radial strips more precisely. The grid systems are shown in Figure 5. Figure 5(a) is viewed in *x-y* plane where the almost black region is the fin surface and the very fine gridlines makes it looked as black. The details of the grid lines in the fin region are shown in Figure 5(c), where it can clearly be seen that the tube boundaries and the strips edges are simulated by stepwise approximations. It should be noted that in order to arrange the pictures conveniently both Figure 5(a) and (b) are not shown in scale. It should be noted that between the fin region and the extended regions the grid spacing change is rather abrupt. A question may arise as whether this may affect the numerical results. A grid comparison was made in He *et al.* (2005) where the same situation happens. And it is found that whether the change in grid spacing is gradual or abrupt is actually has no effect on the heat transfer and fluid flow simulation. This is because in the extended region neither heat transfer nor pressure drop occurs. These two regions are empty and their existence is only for the numerical execution of the inlet and outlet boundary conditions.

Now definitions are presented for the characteristic quantities which will be used in the presentations of numerical results.

Velocity	0.5 m/s		1.0 m/s		1.5 m/s		2.0 m/s		2.5 m/s	
Characteristic parameter	*Nu*	*f*	*Nu*	*f*	*Nu*	*f*	*Nu*	*f*	*Nu*	*f*
Computational value	30.15	3.27	33.81	1.97	36.49	1.58	38.80	1.32	40.71	1.31
Experimental correlations	26.24	3.14	31.78	1.95	36.58	1.53	40.96	1.41	45.04	1.18
Deviation (percent)	+14.9	+4.2	+6.38	+1.2	−2.7	+3.2	−5.3	−7.1	−10.6	+10.6

Table II. Comparison between numerical and experiment results (Kang *et al.*, 1994)

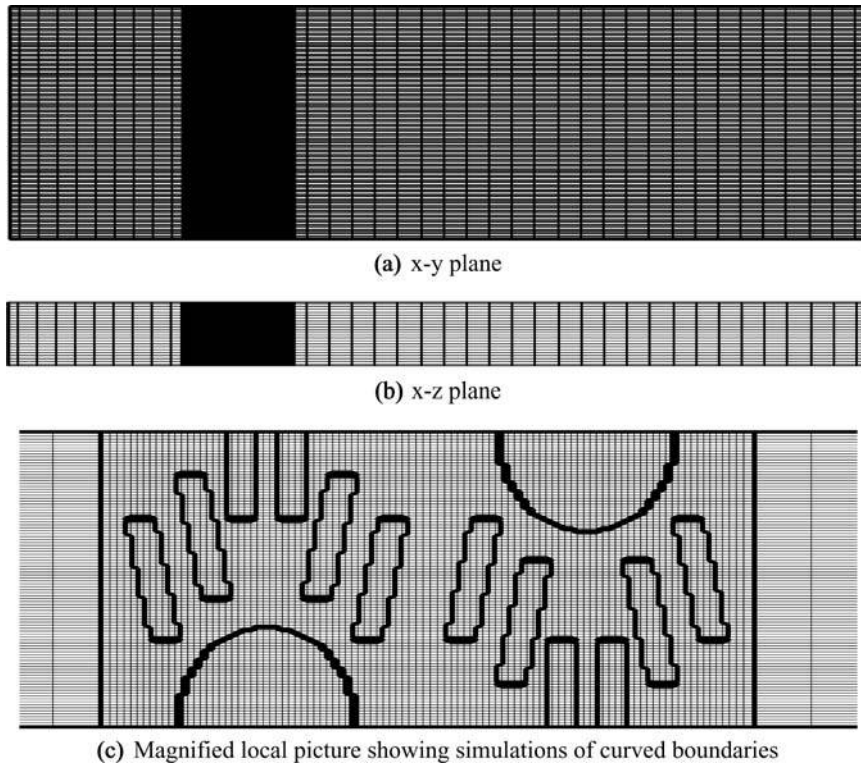

Figure 5.
Grid-system adopted in the simulations

The friction factor is defined by:

$$f = -\frac{\Delta p}{\frac{1}{2}\rho V_{\max}^2 L/d} \tag{1}$$

The Reynolds number and Nusselt numbers are determined by:

$$Re = \frac{V_{\max} d}{\nu}, \quad Nu = \frac{hd}{\lambda} \tag{2a}$$

where

$$h = \frac{Q}{\Delta T_{\lg} A} \tag{2b}$$

In the above definitions, d is the fin collar outside diameter of the tube, $d_o + 2\delta_f$, $V_{\max}$ is the average maximum fluid velocity at the minimum cross section flow area, h is the average heat transfer coefficient of fin surface defined by Newton's law of cooling for which the heat transfer area A is the projection area in the x-y plane of the fin, and $\Delta T_{\lg}$ is the logarithmic mean temperature difference between tube wall and the fluid.

The integration of the convective term in the energy equation over the entire domain is calculated by:

$$I = \int_{\Omega} \rho c_p |\vec{U}| |\mathrm{grad} T| \cos\theta \, d\Omega \tag{3}$$

And the average synergy angle over the entire domain is defined by:

$$\theta_m = \sum \frac{dV_i}{\sum dV_i} \bullet \theta_i \tag{4}$$

In the above equation θ is the local synergy angle between velocity and temperature gradient which is calculated by:

$$\theta = \mathrm{arc}\left(\frac{u\frac{\partial T}{\partial x} + v\frac{\partial T}{\partial y} + w\frac{\partial T}{\partial z}}{|\vec{U}||\mathrm{grad} T|} \right) \tag{5}$$

where u, v, w are the velocity components in x, y, and z directions, respectively.

4. Results and discussion

The presentations of the numerical results will be started from the predicted pressure drop and heat transfer rate in the range of the approaching velocity from 1.0 to 3.0 m/s, followed by the descriptions of flow and temperature fields. Then performance comparisons will be made under the constraint of identical pumping power for the four types of fin surfaces studied. Finally discussion will be conducted from the view point of field synergy principle proposed in Guo *et al.* (1998) and Wang *et al.* (1998).

4.1 Pressure drop and heat transfer results

Figure 6 shows the pressure drop of the four types of fin surface shown in Figure 2. The corresponding frontal velocity ranges from 1.0 to 3.0 m/s. It can be seen that for all types of fin with the increase in flow velocity, the pressure drop increases. The pressure drop also increases with the increase of strip number. The pressure drop of plain plate fin is the lowest among them, and the value of the fully slotted fin is the highest. The pressure drop of the fully slotted fin is about 2.0 times of that of the plain

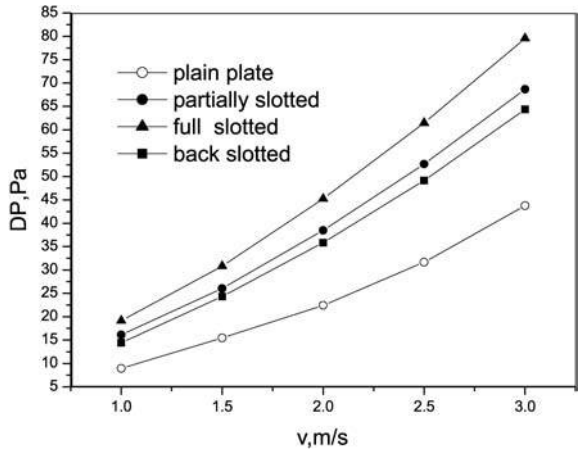

Figure 6.
Pressure drop vs velocity

plate fin at $V = 2.0\,\mathrm{m/s}$. That is mainly due to the frequent interruption of the flow created by the high-density strips. The pressure drop of back slotted fin and partially slotted fin are in the middle of the above two, and the pressure drop of the partially slotted fin is about 7.5 percent higher than that of the back slotted fin at frontal velocity of 2.0 m/s. This is simply because the partially slotted fin has two more strips than that of the back slotted fin.

Figure 7 shows the numerical results of heat transfer rate of the four types of fin at the approaching velocity from 1.0 to 3.0 m/s. The corresponding Reynolds number ranges from 686 to 2,058. The heat transfer rate of all slotted fins is far higher than the plain plate fin, and the more the strips, the higher the heat transfer rate. At the velocity of 2.0 m/s, the heat transfer rate of the fully slotted fin is about 100 percentage higher than that of plain plate fin.

In order to make performance comparison the numerical results are curve-fitted by a quadratic in the form of:

$$Y = A_0 + A_1 X + A_2 X^2 \tag{6}$$

where X stands for the approaching velocity and Y represent friction factor or heat transfer rate. The values of A_0, A_1, A_2 for the different fin surfaces are listed in Table III. The relative deviation of curve-fitting for heat transfer rates and that for pressure drop is very small, being in the order of 10^{-2} ~ 10^{-3}.

In terms of dimensionless parameters, i.e. Reynolds number, friction factor and Nusselt number, the numerical results are shown in Figure 8.

4.2 Flow and temperature fields

The air velocity fields at a *x-y* plane at the middle of *z*-direction are shown in Figure 9. It can be seen that the velocity fields change a lot due to interruption caused by the strips. Compared with the velocity field of the plain plate fin, it can be observed that for the slotted fin surface, the major flow stream after the first cylinder gradually changes its direction with more fluids flow over the area in the back of the second cylinder. Leading to a more uniform flow field in the back part of the fin. This change is, of

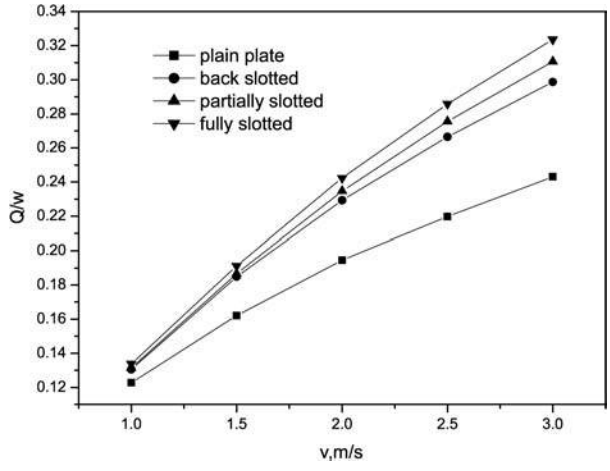

Figure 7.
Heat transfer rate vs velocity

Fin type	Performance	$Y = A_0 + A_1X + A_2X^2$ A_0	A_1	A_2
Plain plate	Dp	3.45938	1.89005	3.82255
	Q	0.03001	0.1043	− 0.01114
Back slotted	Dp	0.13511	10.74531	3.55099
	Q	0.00318	0.14256	− 0.01474
Partially slotted	Dp	1.58148	10.47343	3.96911
	Q	0.0014	0.14366	− 0.01354
Fully slotted	Dp	1.2903	13.55584	4.18554
	Q	− 0.00114	0.14839	− 0.01339

Table III.
Values of A, B1 and B2 in the quadratic

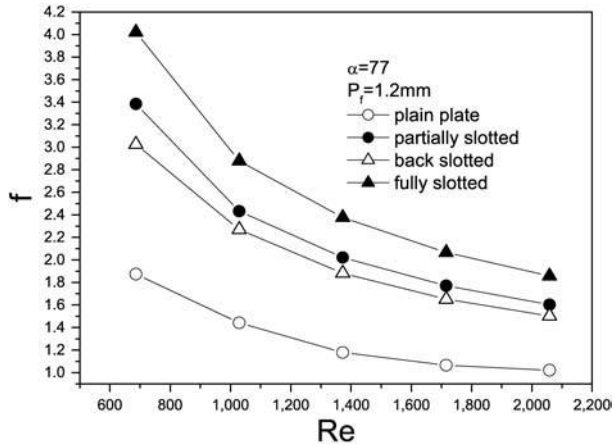

(a) f vs. Re

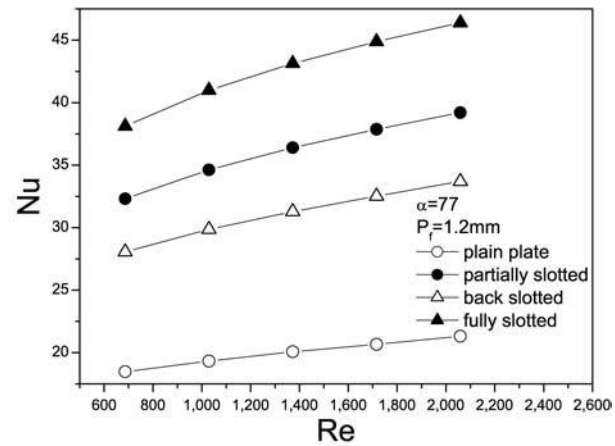

(b) Nu vs. Re

Figure 8.
Variation of friction factor and Nusselt number with *Re*

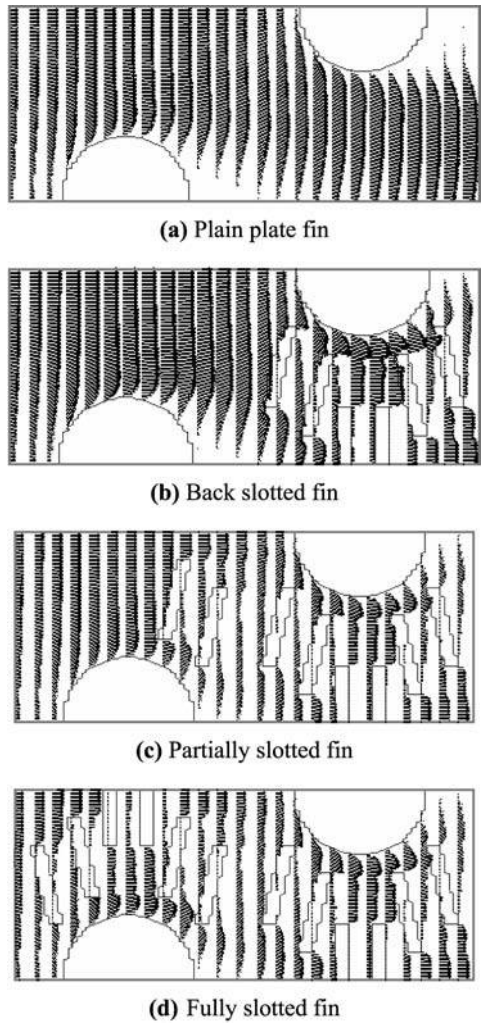

Figure 9.
Air velocity fields in the middle of two adjacent fin surfaces

course, favorable to the enhancement of heat transfer. Therefore, from the conventional point of view of heat transfer augmentation, the enhanced heat transfer rate of the slotted fin surface comes not only from the increase in interruption in the boundary layer, but also the reduction of the void zone in the back of the second cylinder where the velocities are usually quite small and some weak recirculation exists, making this part of surface quite inactive in heat transfer.

The air temperature fields at the middle *x-y* plane are shown in Figure 10. From the isothermal distributions it can be clearly observed that strips appreciably reduce the low temperature region, and the more the strips the larger the region with higher fluid temperature. For the plain plate fin surface, the lowest temperature region penetrates into half of the buffer region between the two cylinders, while for the fully slotted case

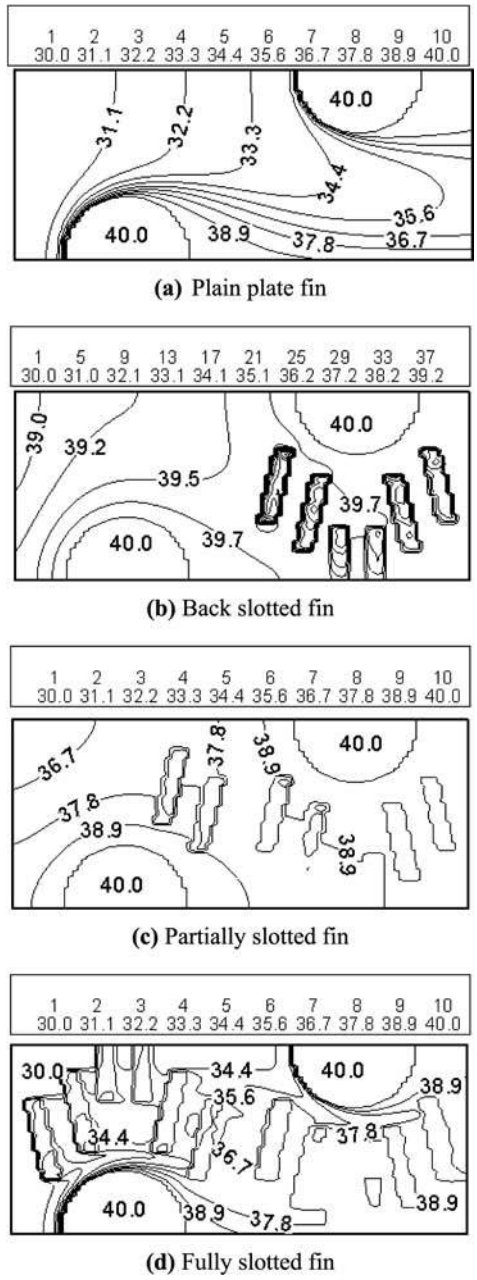

Figure 10.
Air temperature fields in the middle of two adjacent fin surfaces

this low fluid temperature region mainly reduces to the inlet region of the fin surface. This implies that the strips can effectively increase the heat transfer between the surface and the fluid.

4.3 Performance comparisons

From Figures 6-8, it is obvious that the enhancement of heat transfer of the slotted fin surfaces is obtained with the penalty of higher friction factor or pressure drop, and the percentage increase in friction factor even larger than that of Nusselt number. Therefore, a question may arise as how to evaluate the heat transfer and pressure drop performance for such enhanced surface that meaningful conclusion may be obtained. Depending on the objective function, there are a lot of performance evaluation criteria, as discussed in detail in Webb (1994) and Shah and Sekulic (2003). To the authors' opinion, for the air-conditioning engineering, one of the most convenient objectives is to reduce the pumping power for fixed duty and surface area such that the noise and power consumption may be reduced by the adoption of enhanced surface. Therefore, we will adopt the identical pumping power constraint to compare the four types of fin surfaces. According to the geometric conditions in our study, this criterion leading to the following equation (Huang and Tao, 1993):

$$(f\,Re^3)_{\text{plain}} = (f\,Re^3)_{\text{slotted}} \tag{7}$$

The solution process is as follows: starting from a selected Reynolds number of plain plate fin surface, the corresponding value of the Reynolds number of the enhanced surface is searched such that the above equation can be satisfied. In the search process, the curve-fitting equation as shown by equation (6) is used. Therefore, the solution procedure is iterative in nature. Once the pair of the Reynolds numbers of the plain plate fin and the enhance surface are obtained, the corresponding heat transfer rates or the Nusselt numbers can be obtained with ease. The results are shown in Figure 11. It can be seen there that the partially slotted fin surface behaves the best and the heat transfer enhancement of this surface is about 100 percentage higher than that of the plain plate fin within the velocity range compared. This result is quite meaningful and

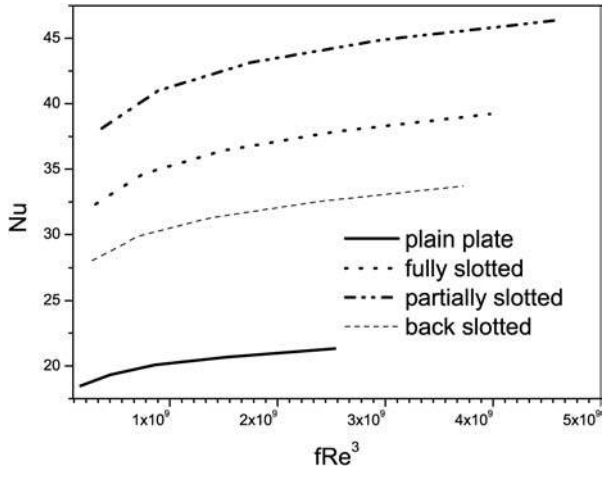

Figure 11.
Comparison under identical pumping power

can explain why in the air-conditioning engineering the slotted fin surface is wide adopted for indoor heat exchangers. What is new in our comparison is that it is the partially slotted surface, not the fully slotted surface that behaves the best. The fully slotted fin surface has too large pressure drop penalty that makes it not so attractive at the constraint of identical pumping power.

Another very simple comparison criterion is the ratio of j factor over friction factor f. Although it is generally not recommended as indicated in Webb (1994), we also adopted this method because its simplicity, and furthermore, for our case it still provides us some useful information. The results are shown in Figure 12. It is interested to see that the partially slotted fin surface almost have the same values of j/f as the fully slotted one.

4.4 Discussion on the mechanism of enhanced heat transfer of slotted fin surface

Attention is now turned to the heat transfer enhancement mechanism of the slotted fin surface. According to brief introduction to the field synergy principle, the domain integration of the convective term equals the overall heat transfer rate, and in our computations it is found that this is the case, with a very small relative difference comes from some numerical errors. The variations of domain integration of the convective term are shown in Figure 13. It can be seen that all the three slotted fin surfaces have much higher values of the integration, which is consistent with Figure 7.

The field synergy principle indicates that the essence to enhance single phase heat transfer is to reduce the synergy angle between the velocity and the temperature gradient. In this paper the domain averaged synergy angle is used as the symbol of synergy between the two fields of the entire domain. It is defined as follows:

$$\theta_m = \sum \frac{dV_i}{\sum dV_i} \bullet \theta_i \tag{8}$$

where θ_i is determined by equation (5).

For the four types of fin studied, at the same frontal velocity the mean synergy angles are compared in Figure 14. Following features may be noted. First the figure

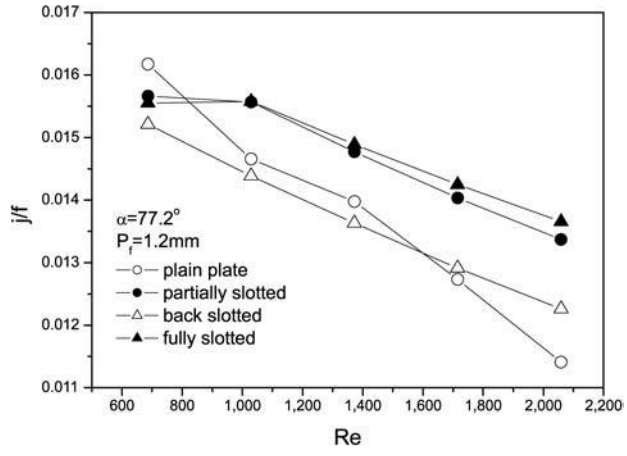

Figure 12.
Comparison of j/f

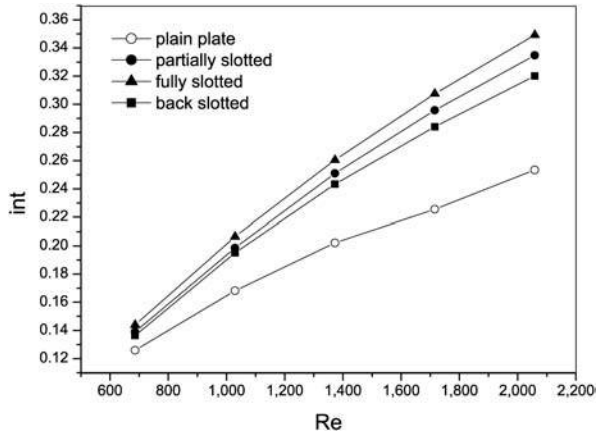

Figure 13.
Domain integral of convective term vs *Re*

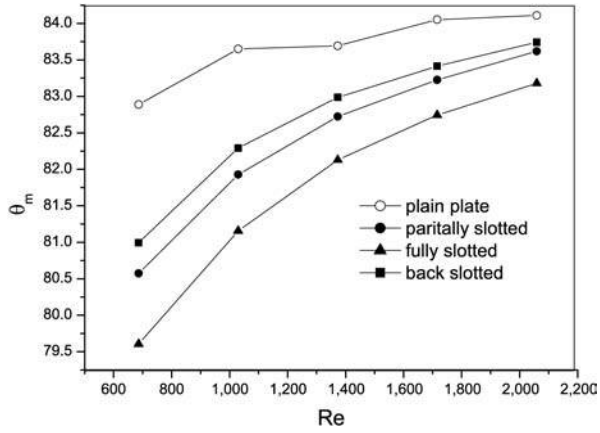

Figure 14.
Domain average synergy angle vs *Re*

shows that the domain average synergy angle becomes larger with the increasing in Re for all the fin surfaces, indicating that the increase in velocity leads to deteriorate the synergy between velocity and temperature gradient; Second, at the same Re, the synergy angles of the slotted fin surfaces all smaller than that of the plain plate fin surface. This implies that the synergy of the slotted fin surface is better than that of the plain plate fin; third, for the three slotted fin surface, the increase in strips leads to the decrease in the synergy angle. Thus it becomes quite clear that the fundamental function of the strips is to improve the synergy of the two fields.

In order to reveal the mechanism in depth, the local synergy angles in the flow field are computed and their distributions are presented for the plain plate fin and the partially slotted fin as examples (Figure 15). It can be observed that at the back of the two cylinders the synergy angles are greatly reduced in the partially slotted fin surface, leading to a better synergy of the whole domain.

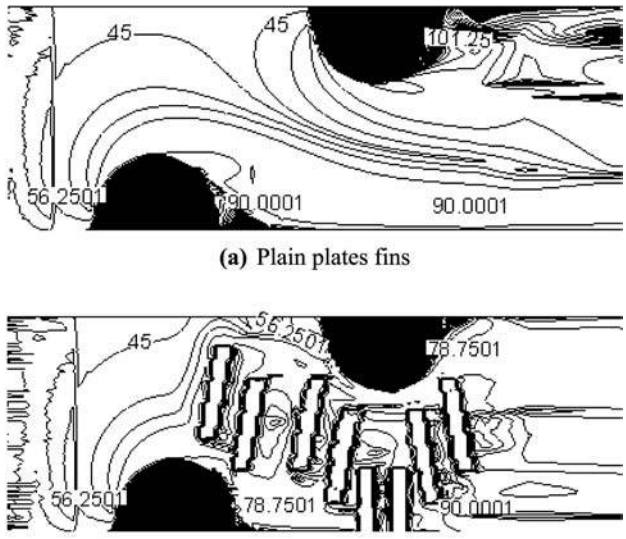

Figure 15.
Local synergy angle field in the middle *x-y* plane

5. Conclusions

According to the above analysis, the following conclusions are drawn:

- For the four types of plate fin surface, both heat transfer and pressure drop increase with the increase of the frontal velocity. At the same frontal velocity, heat transfer rates of the slotted fin surfaces is higher than that of plain plate fin surface. And for the slotted fin with radial strips studied, the more the strips, the higher the heat transfer rate. However, the enhancement of the heat transfer is obtained with larger pressure drop penalty. In the range of velocity computed, the corresponding equations for the heat transfer rates and pressure drop with the frontal velocity are obtained.
- Performance comparison under the identical pumping power indicates that the partially slotted fin surface has the best performance. The major character of the partially slotted fin surface is that the strips are mainly located in the downstream part of the fin, with no strips arranged in the inlet part of the fin. The j over f ratio of the partially slotted fin surface is almost the same as that of the fully slotted one within the entire range of the approaching velocity.
- Analysis from the view point of field synergy principle demonstrates that the strips of the slotted fin surface can appreciably reduce the domain average synergy angle between velocity and temperature gradient, hence improve the synergy between the two fields. The slots located at the back of cylinder where vortex usually occurs can significantly reduce the local intersection angle.

The above results should be useful for the design of new type of enhanced surface.

References

Atkinson, K.N., Drakulic, R. and Cowell, A. *et al.* (1998), "Two- and three-dimensional numerical models of flow and heat transfer over louvered fin arrays in compact heat exchangers", *International Journal of Heat and Mass Transfer*, Vol. 41, pp. 4063-80.

Comini, G. and Groce, G. (2001), "Convective heat mass transfer in tube-fin exchangers under dehumidifying conditions", *Numerical Heat Transfer. Part A*, Vol. 40, pp. 579-99.

Guo, Z.Y., Li, D.Y. and Wang, B.X. (1998), "A novel concept for convective heat transfer enhancement [J]", *International Journal of Heat and Mass Transfer*, Vol. 41, pp. 2221-5.

He, Y.L., Tao, W.Q., Song, F.Q. and Zhang, W. (2005), "Three-dimensional numerical study of heat transfer characteristics of plain plate fin-and-tube heat exchangers from view point of field synergy principle", *International Journal of Heat & Fluid Flow*, Vol. 26, pp. 459-473.

Huang, H.Z. and Tao, W.Q. (1993), "An experimental study on heat transfer and pressure drop characteristics of arrays of non-uniform plate length positioned obliquely to the flow direction", *ASME Journal of Heat Transfer*, Vol. 115 No. 3, pp. 568-75.

Jing, C.M. and Ralphl, W. (2001), "Numerical predictions of Wavy fin coil performance", *Enhanced Heat Transfer*, pp. 159-73.

Kang, H.J., Li, W., Li, H.J., Xin, R.C. and Tao, W.Q. (1994), "Experimental study on heat transfer and pressure drop characteristics of four types of plate fin-and-tube heat exchanger surfaces", *International Journal of Thermal and Fluid Science*, Vol. 3 No. 1, pp. 34-42.

Kays, W.M. and London, A.L. (1984), *Compact Heat Exchangers*, 3rd ed., McGraw-Hill, New York, NY.

Leu, J.S., Liu, M.S., Liaw, J.S. and Wang, C.C. (2001), "A numerical investigation of louvered fin-and-tube heat exchangers having circular and oval tube configuration", *International Journal of Heat and Mass Transfer*, Vol. 44, pp. 4235-43.

Mori, Y. and Nakayama, W. (1982), "Recent advances incompact heat exchangers in Japan", ASME HTD-10.

Patankar, S.V. (1980), *Numerical Heat Transfer and Fluid Flow*, McGraw-Hill, New York, NY.

Shah, R.K. and Sekulic, D.P. (2003), *Fundamentals of Heat Exchanger Design*, Chapter 10, Wiley, New York, NY.

Shah, R.K., Heikal, M.R., Thonon, B. and Tochon, P. (2001), "Progress in the numerical analysis of compact heat exchanger surfaces", *Advances in Heat Transfer*, Academic Press, New York, NY, Vol. 34, pp. 363-442.

Tao, W.Q. (2000), *Recent Advances of Numerical Heat Transfer [M]*, Science Publish House, Beijing.

Tao, W.Q. (2001), *Numerical Heat Transfer*, 2nd ed., Xi'an Jiaotong University Press, Xi'an.

Tao, W.Q., Guo, Z.Y. and Wang, B.X. (2002a), "Field synergy principle for enhancing convective heat transfer its extension and numerical verifications", *International Journal of Heat and Mass Transfer*, Vol. 45, pp. 849-56.

Tao, W.Q., He, Y.L., Wang, Q.W., Qu, Z.G. and Song, F.Q. (2002b), "A unified analysis on enhancing single phase convective heat transfer with field synergy principle", *International Journal of Heat and Mass Transfer*, Vol. 45, pp. 4871-9.

Wang, S., Li, Z.X. and Guo, Z.Y. (1998), "Novel concept and device of heat transfer augmentation", *Proceeedings of 11th International Heat Transfer Conference*, Vol. 5, pp. 405-8.

Wang, C.C., Lee, W.S. and Sheu, W.J.A. (2001), "Comparative study of compact enhanced fin-and-tube heat exchangers heat exchangers", *International Journal of Heat and Mass Transfer*, Vol. 44, pp. 3565-73.

Webb, R.L. (1994), *Principles of Enhanced Heat Transfer*, Chapter 3, Wiley, New York, NY.

Xin, R.C., Li, H.Z., Kang, H.J., Li, W. and Tao, W.Q. (1992), "Heat transfer and pressure drop measurement on four types of plate-fin-and-tube heat exchanger surfaces", in Wang, B.X. (Ed.), *Transport Phenomena: Science and Technology, 1992*, Higher Education Press, Beijing, pp. 942-7.

Zhou, J.J., Tao, W.Q. and He, Y.L. (2003), "Numerical simulation of heat transfer performance of slotted fin surface", paper presented at the International Conference on Cryogenics and Refrigeration, Cryogenics and Refrigeration – (ICCR 2003)[C], 22-25 April, pp. 540-3.

This article has been cited by:

1. Xiao-Yu Li, Zhao-Hui Li, Wen-Quan Tao. 2018. Experimental study on heat transfer and pressure drop characteristics of fin-and-tube surface with four convex-strips around each tube. *International Journal of Heat and Mass Transfer* **116**, 1085-1095. [Crossref]
2. Yu Wang, Ya-Ling He, Yin-Shi Li, Ze-Dong Cheng. 2016. Theoretical study of air-side volatility effects on the performance of H-type finned heat exchangers in waste heat utilization. *Numerical Heat Transfer, Part A: Applications* **70**:6, 613-638. [Crossref]
3. Y.Q. Kong, L.J. Yang, X.Z. Du, Y.P. Yang. 2016. Air-side flow and heat transfer characteristics of flat and slotted finned tube bundles with various tube pitches. *International Journal of Heat and Mass Transfer* **99**, 357-371. [Crossref]
4. Yu Jin, Zhi-Qiang Yu, Gui-Hua Tang, Ya-Ling He, Wen-Quan Tao. 2016. Parametric study and multiple correlations of an H-type finned tube bank in a fully developed region. *Numerical Heat Transfer, Part A: Applications* **70**:1, 64-78. [Crossref]
5. Y.Q. Kong, L.J. Yang, X.Z. Du, Y.P. Yang. 2016. Effects of continuous and alternant rectangular slots on thermo-flow performances of plain finned tube bundles in in-line and staggered configurations. *International Journal of Heat and Mass Transfer* **93**, 97-107. [Crossref]
6. Ya-Ling He, Wen-Quan Tao. Convective Heat Transfer Enhancement: Mechanisms, Techniques, and Performance Evaluation 87-186. [Crossref]
7. Yu Jin, Gui-Hua Tang, Ya-Ling He, Wen-Quan Tao. 2013. Parametric study and field synergy principle analysis of H-type finned tube bank with 10 rows. *International Journal of Heat and Mass Transfer* **60**, 241-251. [Crossref]
8. Vladimir Glazar, Anica Trp, Kristian Lenic. 2012. Numerical Study of Heat Transfer and Analysis of Optimal Fin Pitch in a Wavy Fin-and-Tube Heat Exchanger. *Heat Transfer Engineering* **33**:2, 88-96. [Crossref]
9. Ju-Fang Fan, Ya-Ling He, Wen-Quan Tao. 2012. Application of Combined Enhanced Techniques for Design of Highly Efficient Air Heat Transfer Surface. *Heat Transfer Engineering* **33**:1, 52-62. [Crossref]
10. R.J. Goldstein, W.E. Ibele, S.V. Patankar, T.W. Simon, T.H. Kuehn, P.J. Strykowski, K.K. Tamma, J.V.R. Heberlein, J.H. Davidson, J. Bischof, F.A. Kulacki, U. Kortshagen, S. Garrick, V. Srinivasan, K. Ghosh, R. Mittal. 2010. Heat transfer—A review of 2005 literature. *International Journal of Heat and Mass Transfer* **53**:21-22, 4397-4447. [Crossref]
11. Jian-Fei Zhang, Ya-Ling He, Wen-Quan Tao. 2009. 3D numerical simulation on shell-and-tube heat exchangers with middle-overlapped helical baffles and continuous baffles – Part II: Simulation results of periodic model and comparison between continuous and noncontinuous helical baffles. *International Journal of Heat and Mass Transfer* **52**:23-24, 5381-5389. [Crossref]
12. Gongnan Xie, Qiuwang Wang, Bengt Sunden. 2009. Parametric study and multiple correlations on air-side heat transfer and friction characteristics of fin-and-tube heat exchangers with large number of large-diameter tube rows. *Applied Thermal Engineering* **29**:1, 1-16. [Crossref]